

TOPOLOGICAL SENSITIVITY ANALYSIS FOR INCLUSION IN TWO-DIMENSIONAL LINEAR ELASTICITY PROBLEM

S.M. GIUSTI, A.A. NOVOTNY, AND C. PADRA

ABSTRACT. The topological derivative gives the sensitivity of the problem when the domain under consideration is perturbed by the introduction of a hole. Alternatively, this same concept can also be used to calculate the sensitivity of the problem when, instead of a hole, a small inclusion is introduced at a point in the domain. In the present paper we apply the Topological-Shape Sensitivity Method to obtain the topological derivative for inclusion in two-dimensional linear elasticity problems, adopting the total potential energy as the cost function and the equilibrium equation as a constraint. For the sake of completeness, initially we present a brief description of the Topological-Shape Sensitivity Method. Then, we calculate the topological derivative for the problem under consideration in two steps: firstly we perform the shape derivative and next we calculate the limit when the perturbation vanishes using classical asymptotic analysis around a circular inclusion. In addition, we use this information as a descent direction in a topology design algorithm which allows to simultaneously remove and insert material. Finally, we explore this feature showing some numerical experiments of structural topology design within the context of two-dimensional linear elasticity problem.

1. INTRODUCTION

As it is understood, the topological derivative furnishes the sensitivity of the problem when the domain under consideration is perturbed by the introduction of a hole [8, 9, 26, 29]. This methodology has been recognized as an alternative and at the same time a promising tool to solve topology optimization problems (see, for instance, [10] and references therein). Moreover, this is a broad concept. In fact, the topological derivative may also be applied to analyze any kind of sensitivity problem in which, instead of a hole, discontinuous changes defined in an infinitesimal region are allowable; for example, discontinuous changes on the shape of the boundary, on the boundary conditions, on the load system and/or on the parameters of the problem. In particular when the parameter is related to material property, we can calculate the topological derivative for inclusion [25], instead of a hole.

Therefore, the information provided by the topological derivative is also very effective to solve problems such as image processing (enhancement and segmentation) [4, 5, 20, 21], inverse problems (domain, boundary conditions and parameters characterization) [3, 6, 7, 14, 19, 23] and in the mechanical modeling of problems with changes on the configuration of the domain like fracture mechanics and damage.

Several methods were proposed to calculate the topological derivative [1, 8, 25, 29]. In the present work we extend the application of the Topological-Shape Sensitivity Method developed in [25] to obtain the topological derivative for inclusion in two-dimensional linear elasticity problems, adopting the total potential energy as the cost function and the equilibrium equation as the constraint. Next, we apply this result to devise a topology design algorithm which allows us to simultaneously remove and insert material. This feature is demonstrated in numerical experiments that we exhibit.

This study is organized in the following manner. In section 2, we present a brief description of the Topological-Shape Sensitivity Method. In section 3, we calculate the topological derivative for inclusion for the problem under consideration. Lastly, in section 4, we show some numerical results concerning structural topology design.

Key words and phrases. topological derivative for inclusion, shape sensitivity analysis, topology design, asymptotic analysis.

2. TOPOLOGICAL-SHAPE SENSITIVITY METHOD

Let us consider an open bounded domain $\Omega \subset \mathbb{R}^2$ with a smooth boundary $\partial\Omega$. If the domain Ω is perturbed by introducing a small inclusion represented by B_ε , which is a ball of radius ε centered at point $\hat{\mathbf{x}} \in \Omega$, we have a perturbed domain $\Omega_\varepsilon \cup B_\varepsilon$, where $\Omega_\varepsilon = \Omega - B_\varepsilon$, as shown in fig. (1). Thus, considering a cost function ψ defined in both domains Ω and $\Omega_\varepsilon \cup B_\varepsilon$, its topological derivative is written as

$$D_T(\hat{\mathbf{x}}) = \lim_{\varepsilon \rightarrow 0} \frac{\psi(\Omega_\varepsilon \cup B_\varepsilon) - \psi(\Omega)}{f(\varepsilon)}, \quad (1)$$

where $f(\varepsilon)$ is a function that decreases monotonically so that $f(\varepsilon) \rightarrow 0$ with $\varepsilon \rightarrow 0^+$.

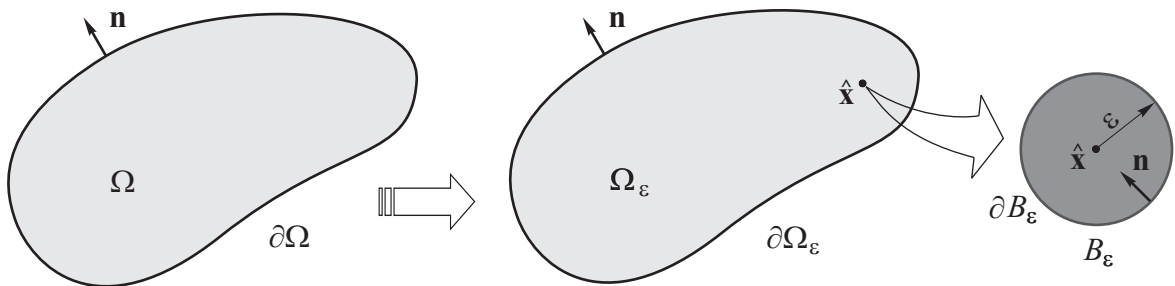


FIGURE 1. Topological derivative concept.

Recently an alternative procedure to calculate the topological derivative, called Topological-Shape Sensitivity Method, have been introduced by the authors (see, for instance, [12, 26]). This approach makes use of the whole mathematical framework (and results) developed for shape sensitivity analysis (see, for instance, the pioneering work of Murat & Simon [24]). The main result obtained in [12, 26] may be briefly summarized in the following Theorem (see also [25]):

Theorem 1. : *Let $f(\varepsilon)$ be a function chosen in order to $0 < |D_T(\hat{\mathbf{x}})| < \infty$, then the topological derivative given by eq. (1) can be written as*

$$D_T(\hat{\mathbf{x}}) = \lim_{\varepsilon \rightarrow 0} \frac{1}{f'(\varepsilon)} \left. \frac{d}{d\tau} \psi(\Omega_\tau) \right|_{\tau=0}, \quad (2)$$

where $\tau \in \mathbb{R}^+$ is used to parameterize the domain. That is, for τ small enough, we have

$$\Omega_\tau := \{ \mathbf{x}_\tau \in \mathbb{R}^2 : \mathbf{x}_\tau = \mathbf{x} + \tau \mathbf{v}, \mathbf{x} \in \Omega_\varepsilon \cup B_\varepsilon \}. \quad (3)$$

Therefore, $\mathbf{x}_\tau|_{\tau=0} = \mathbf{x}$ and $\Omega_\tau|_{\tau=0} = \Omega_\varepsilon \cup B_\varepsilon$. In addition, considering that \mathbf{n} is the outward normal unit vector (see fig. 1), then we can define the shape change velocity \mathbf{v} , which is a smooth vector field in $\Omega_\varepsilon \cup B_\varepsilon$ assuming the following values on the boundary ∂B_ε and $\partial\Omega$

$$\begin{cases} \mathbf{v} = -\mathbf{n} & \text{on } \partial B_\varepsilon \\ \mathbf{v} = \mathbf{0} & \text{on } \partial\Omega \end{cases} \quad (4)$$

and the shape sensitivity of the cost function in relation to the domain perturbation characterized by \mathbf{v} is given by

$$\left. \frac{d}{d\tau} \psi(\Omega_\tau) \right|_{\tau=0} = \lim_{\tau \rightarrow 0} \frac{\psi(\Omega_\tau) - \psi(\Omega_\varepsilon \cup B_\varepsilon)}{\tau}. \quad (5)$$

Proof. The reader interested in the proof of this result may refer to [12, 25, 26]. \square

3. THE TOPOLOGICAL DERIVATIVE FOR INCLUSION

To highlight the potentialities of the Topological-Shape Sensitivity Method, it will be applied to calculate the topological derivative for inclusion in two-dimensional linear elasticity problems considering the total potential energy as the cost function and the equilibrium equation in its weak form as the constraint. Therefore, considering the above problem, initially we perform the shape sensitivity of the adopted cost function with respect to the shape change of the inclusion and lastly we calculate the associated topological derivative.

3.1. Shape sensitivity analysis . Let us choose the total potential energy stored in the elastic solid under analysis as the cost function. For simplicity, we assume that the external load remains fixed during the shape change. As it is well-known, different approaches can be applied to obtain the shape derivative of the cost function. However, in our particular case, as the cost function is associated with the potential of the state equation, the direct differentiation method will be adopted to calculate its shape derivative. Therefore, considering the total potential energy already written in the configuration Ω_τ , eq. (3), then $\psi(\Omega_\tau) := \mathcal{J}_{\Omega_\tau}(\mathbf{u}_\tau) : \mathcal{U}_\tau \mapsto \mathbb{R}$ can be expressed by

$$\mathcal{J}_{\Omega_\tau}(\mathbf{u}_\tau) = \frac{1}{2} \int_{\Omega_\tau} \mathbf{T}_\tau(\mathbf{u}_\tau) \cdot \mathbf{E}_\tau(\mathbf{u}_\tau) d\Omega_\tau - \int_{\Gamma_N} \bar{\mathbf{q}} \cdot \mathbf{u}_\tau d\Gamma_\tau, \quad (6)$$

where the admissible displacements set \mathcal{U}_τ is given by

$$\mathcal{U}_\tau = \{ \mathbf{u}_\tau \in H^1(\Omega_\tau) : \mathbf{u}_\tau = \bar{\mathbf{u}} \text{ on } \Gamma_D \}. \quad (7)$$

The strain and stress tensors $\mathbf{E}_\tau(\mathbf{u}_\tau)$ and $\mathbf{T}_\tau(\mathbf{u}_\tau)$ are respectively given by

$$\mathbf{E}_\tau(\mathbf{u}_\tau) = \nabla_\tau^s \mathbf{u}_\tau \quad \text{and} \quad \mathbf{T}_\tau(\mathbf{u}_\tau) = \mathbf{C}_\delta \nabla_\tau^s \mathbf{u}_\tau, \quad (8)$$

with $\nabla_\tau(\cdot)$ used to denote

$$\nabla_\tau(\cdot) := \frac{\partial}{\partial \mathbf{x}_\tau}(\cdot), \quad (9)$$

and the elasticity tensor \mathbf{C}_δ is defined as following

$$\mathbf{C}_\delta = \frac{K_\delta}{1 - \nu^2} [(1 - \nu) \mathbf{I} + \nu (\mathbf{I} \otimes \mathbf{I})] \quad (10)$$

where \mathbf{I} and \mathbf{II} are respectively the second and fourth order identity tensors, ν is the Poisson's ratio and, for $\delta \in \mathbb{R}^+$, K_δ is the Young's modulus given by

$$K_\delta = \begin{cases} K & \text{if } \mathbf{x} \in \Omega_\varepsilon \\ \delta K & \text{if } \mathbf{x} \in B_\varepsilon \end{cases} \quad (11)$$

In addition, \mathbf{u}_τ is the solution of the variational problem defined in the configuration Ω_τ , that is: find the displacement vector field $\mathbf{u}_\tau \in \mathcal{U}_\tau$ such that

$$\int_{\Omega_\tau} \mathbf{T}_\tau(\mathbf{u}_\tau) \cdot \mathbf{E}_\tau(\boldsymbol{\eta}_\tau) d\Omega_\tau = \int_{\Gamma_N} \bar{\mathbf{q}} \cdot \boldsymbol{\eta}_\tau d\Gamma_\tau \quad \forall \boldsymbol{\eta}_\tau \in \mathcal{V}_\tau, \quad (12)$$

where

$$\mathcal{V}_\tau = \{ \boldsymbol{\eta}_\tau \in H^1(\Omega_\tau) : \boldsymbol{\eta}_\tau = \mathbf{0} \text{ on } \Gamma_D \}. \quad (13)$$

Observe that from the well-known terminology of Continuum Mechanics, the domains $\Omega_\tau|_{\tau=0} = \Omega_\varepsilon \cup B_\varepsilon$ and Ω_τ can be interpreted as the material and the spatial configurations, respectively. Therefore, in order to calculate the shape derivative of the cost function $\mathcal{J}_{\Omega_\tau}(\mathbf{u}_\tau)$, at $\tau = 0$, we may use the Reynolds' transport theorem and the concept of material derivatives of spatial fields, that is [17]

$$\frac{d}{d\tau} \int_{\Omega_\tau} \varphi_\tau \Big|_{\tau=0} = \int_{\Omega_\varepsilon \cup B_\varepsilon} (\dot{\varphi}_\tau|_{\tau=0} + \varphi_\tau|_{\tau=0} \operatorname{div} \mathbf{v}) d\Omega_\varepsilon, \quad (14)$$

where φ_τ is a spatial scalar field and $(\dot{\cdot})$ is used to denote

$$(\dot{\cdot}) := \frac{d(\cdot)}{d\tau}. \quad (15)$$

Taking into account the cost function defined through eq. (6) and assuming that the parameters K , ν , $\bar{\mathbf{u}}$, and $\bar{\mathbf{q}}$ are constants in relation to the perturbation represented by τ , we have, from eq. (14) and following Theorem 1, eqs. (3,4), that

$$\begin{aligned} \left. \frac{d}{d\tau} \mathcal{J}_{\Omega_\tau}(\mathbf{u}_\tau) \right|_{\tau=0} &= \frac{1}{2} \int_{\Omega_\varepsilon \cup B_\varepsilon} \left[\left. \frac{d}{d\tau} (\mathbf{T}_\tau(\mathbf{u}_\tau) \cdot \mathbf{E}_\tau(\mathbf{u}_\tau)) \right|_{\tau=0} + \mathbf{T}_\varepsilon(\mathbf{u}_\varepsilon) \cdot \mathbf{E}_\varepsilon(\mathbf{u}_\varepsilon) \operatorname{div} \mathbf{v} \right] d\Omega_\varepsilon \\ &\quad - \int_{\Gamma_N} \bar{\mathbf{q}} \cdot \dot{\mathbf{u}}_\varepsilon d\Gamma_\varepsilon, \end{aligned} \quad (16)$$

where, according to the material derivatives of spatial fields [17], we have

$$\left. \frac{d}{d\tau} (\mathbf{T}_\tau(\mathbf{u}_\tau) \cdot \mathbf{E}_\tau(\mathbf{u}_\tau)) \right|_{\tau=0} = 2 (\mathbf{T}_\varepsilon(\mathbf{u}_\varepsilon) \cdot \mathbf{E}_\varepsilon(\dot{\mathbf{u}}_\varepsilon) - \mathbf{T}_\varepsilon(\mathbf{u}_\varepsilon) \cdot (\nabla \mathbf{u}_\varepsilon \nabla \mathbf{v})^s). \quad (17)$$

Substituting eq. (17) in eq. (16) we obtain

$$\begin{aligned} \left. \frac{d}{d\tau} \mathcal{J}_{\Omega_\tau}(\mathbf{u}_\tau) \right|_{\tau=0} &= \int_{\Omega_\varepsilon \cup B_\varepsilon} \left[\frac{1}{2} \mathbf{T}_\varepsilon(\mathbf{u}_\varepsilon) \cdot \mathbf{E}_\varepsilon(\mathbf{u}_\varepsilon) \operatorname{div} \mathbf{v} - \mathbf{T}_\varepsilon(\mathbf{u}_\varepsilon) \cdot (\nabla \mathbf{u}_\varepsilon \nabla \mathbf{v})^s \right] d\Omega_\varepsilon \\ &\quad + \int_{\Omega_\varepsilon \cup B_\varepsilon} \mathbf{T}_\varepsilon(\mathbf{u}_\varepsilon) \cdot \mathbf{E}_\varepsilon(\dot{\mathbf{u}}_\varepsilon) d\Omega_\varepsilon - \int_{\Gamma_N} \bar{\mathbf{q}} \cdot \dot{\mathbf{u}}_\varepsilon d\Gamma_\varepsilon. \end{aligned} \quad (18)$$

Since \mathbf{u}_ε is the solution of the variational problem given by eq. (12) for $\tau = 0$ and considering that $\dot{\mathbf{u}}_\varepsilon \in \mathcal{V}_\varepsilon$, eq. (18) becomes

$$\left. \frac{d}{d\tau} \mathcal{J}_{\Omega_\tau}(\mathbf{u}_\tau) \right|_{\tau=0} = \int_{\Omega_\varepsilon \cup B_\varepsilon} \boldsymbol{\Sigma}_\varepsilon \cdot \nabla \mathbf{v} d\Omega_\varepsilon, \quad (19)$$

where $\boldsymbol{\Sigma}_\varepsilon$ is the Eshelby energy-momentum tensor (see, for instance, [11, 18, 30]) given in this particular case by

$$\boldsymbol{\Sigma}_\varepsilon = \frac{1}{2} (\mathbf{T}_\varepsilon(\mathbf{u}_\varepsilon) \cdot \mathbf{E}_\varepsilon(\mathbf{u}_\varepsilon)) \mathbf{I} - (\nabla \mathbf{u}_\varepsilon)^T \mathbf{T}_\varepsilon(\mathbf{u}_\varepsilon). \quad (20)$$

Taking into account eq. (19) and considering the tensorial relation

$$\operatorname{div}(\boldsymbol{\Sigma}_\varepsilon^T \mathbf{v}) = \boldsymbol{\Sigma}_\varepsilon \cdot \nabla \mathbf{v} + \operatorname{div} \boldsymbol{\Sigma}_\varepsilon \cdot \mathbf{v}, \quad (21)$$

we can apply the divergence theorem to obtain

$$\left. \frac{d}{d\tau} \mathcal{J}_{\Omega_\tau}(\mathbf{u}_\tau) \right|_{\tau=0} = \int_{\partial\Omega} \boldsymbol{\Sigma}_\varepsilon \mathbf{n} \cdot \mathbf{v} d\partial\Omega + \int_{\partial B_\varepsilon} \llbracket \boldsymbol{\Sigma}_\varepsilon \mathbf{n} \rrbracket \cdot \mathbf{v} d\partial B_\varepsilon - \int_{\Omega_\varepsilon \cup B_\varepsilon} \operatorname{div} \boldsymbol{\Sigma}_\varepsilon \cdot \mathbf{v} d\Omega_\varepsilon. \quad (22)$$

In addition, it is straightforward to verify that, in this particular case, the Eshelby tensor has null divergence, that is $\operatorname{div} \boldsymbol{\Sigma}_\varepsilon = \mathbf{0}$. Therefore, the shape derivative of the cost function $\mathcal{J}_{\Omega_\tau}(\mathbf{u}_\tau)$ defined through eq. (6), at $\tau = 0$, becomes an integral defined on the boundary ∂B_ε since $\mathbf{v} = 0$ on $\partial\Omega$ (see eq. 4), that is,

$$\left. \frac{d}{d\tau} \mathcal{J}_{\Omega_\tau}(\mathbf{u}_\tau) \right|_{\tau=0} = \int_{\partial B_\varepsilon} \llbracket \boldsymbol{\Sigma}_\varepsilon \mathbf{n} \rrbracket \cdot \mathbf{v} d\partial B_\varepsilon. \quad (23)$$

In other words, the shape sensitivity of the cost functional only depends on the jump of the Eshelby tensor through the boundary ∂B_ε .

3.2. Topological sensitivity analysis . In order to calculate the topological derivative for inclusion using the Topological-Shape Sensitivity Method, we substitute eq. (23) in the result of Theorem 1 (eq. 2). Therefore, from the definition of the velocity field (eq. 4) and considering the shape derivative of the cost function (eq. 23), we have

$$\left. \frac{d}{d\tau} \mathcal{J}_{\Omega_\tau}(\mathbf{u}_\tau) \right|_{\tau=0} = - \int_{\partial B_\varepsilon} \llbracket \boldsymbol{\Sigma}_\varepsilon \mathbf{n} \rrbracket \cdot \mathbf{n} d\partial B_\varepsilon. \quad (24)$$

Considering a curvilinear coordinate system defined on the boundary ∂B_ε , the stress tensor $\mathbf{T}_\varepsilon(\mathbf{u}_\varepsilon)$ and the strain tensor $\mathbf{E}_\varepsilon(\mathbf{u}_\varepsilon)$, when defined on the boundary ∂B_ε , can be decomposed in the following way

$$\mathbf{T}_\varepsilon(\mathbf{u}_\varepsilon)|_{\partial B_\varepsilon} = T_\varepsilon^{nn}(\mathbf{n} \otimes \mathbf{n}) + T_\varepsilon^{nt}(\mathbf{n} \otimes \mathbf{t}) + T_\varepsilon^{tn}(\mathbf{t} \otimes \mathbf{n}) + T_\varepsilon^{tt}(\mathbf{t} \otimes \mathbf{t}), \quad (25)$$

$$\mathbf{E}_\varepsilon(\mathbf{u}_\varepsilon)|_{\partial B_\varepsilon} = E_\varepsilon^{nn}(\mathbf{n} \otimes \mathbf{n}) + E_\varepsilon^{nt}(\mathbf{n} \otimes \mathbf{t}) + E_\varepsilon^{tn}(\mathbf{t} \otimes \mathbf{n}) + E_\varepsilon^{tt}(\mathbf{t} \otimes \mathbf{t}), \quad (26)$$

where \mathbf{n} and \mathbf{t} are respectively the normal and tangential unit vectors ($\mathbf{n} \cdot \mathbf{t} = 0$) defined on ∂B_ε . Thus, the jump condition on the boundary ∂B_ε can be written as

$$\begin{aligned} \llbracket \mathbf{T}_\varepsilon(\mathbf{u}_\varepsilon) \mathbf{n} \rrbracket &= (T_\varepsilon^{nn}|_e - T_\varepsilon^{nn}|_i) \mathbf{n} + (T_\varepsilon^{tn}|_e - T_\varepsilon^{tn}|_i) \mathbf{t} = \mathbf{0} \\ \Rightarrow T_\varepsilon^{nn}|_e &= T_\varepsilon^{nn}|_i \quad \text{and} \quad T_\varepsilon^{tn}|_e = T_\varepsilon^{tn}|_i \quad \text{on } \partial B_\varepsilon. \end{aligned} \quad (27)$$

In the same way, the displacement field \mathbf{u}_ε defined on the boundary ∂B_ε can be decomposed as

$$\mathbf{u}_\varepsilon|_{\partial B_\varepsilon} = u_\varepsilon^n \mathbf{n} + u_\varepsilon^t \mathbf{t}. \quad (28)$$

Therefore, its continuity condition results in

$$\llbracket \mathbf{u}_\varepsilon \rrbracket = \mathbf{0} \quad \Rightarrow \quad \mathbf{u}_\varepsilon|_e = \mathbf{u}_\varepsilon|_i \quad \text{and} \quad \left. \frac{\partial(\cdot)}{\partial t} \right|_e = \left. \frac{\partial(\cdot)}{\partial t} \right|_i \quad \text{on } \partial B_\varepsilon, \quad (29)$$

or in terms of the strain tensor components, we have

$$E_\varepsilon^{tt}|_e = E_\varepsilon^{tt}|_i. \quad (30)$$

Using the decompositions defined through eqs. (25, 26, 28), the Eshelby tensor flux in the normal direction is given by

$$\begin{aligned} \Sigma_\varepsilon \mathbf{n} \cdot \mathbf{n} &= \frac{1}{2} (\mathbf{T}_\varepsilon(\mathbf{u}_\varepsilon) \cdot \mathbf{E}_\varepsilon(\mathbf{u}_\varepsilon)) - \mathbf{T}_\varepsilon(\mathbf{u}_\varepsilon) \mathbf{n} \cdot (\nabla \mathbf{u}_\varepsilon) \mathbf{n} \\ &= \frac{1}{2} \left[T_\varepsilon^{tt} E_\varepsilon^{tt} - T_\varepsilon^{nn} E_\varepsilon^{nn} + T_\varepsilon^{tn} \left(\frac{\partial u_\varepsilon^n}{\partial t} - \frac{\partial u_\varepsilon^t}{\partial n} \right) \right]. \end{aligned} \quad (31)$$

From the jump and continuity conditions on the boundary ∂B_ε given by eqs. (27, 29, 30) and considering the constitutive relation given by eq. (8) for $\tau = 0$, the jump of the Eshelby tensor flux in the normal direction results in

$$\begin{aligned} \llbracket \Sigma_\varepsilon \mathbf{n} \rrbracket \cdot \mathbf{n} &= (\Sigma_\varepsilon|_e - \Sigma_\varepsilon|_i) \mathbf{n} \cdot \mathbf{n} \\ &= \frac{1}{2} \left[(T_\varepsilon^{tt}|_e - T_\varepsilon^{tt}|_i) E_\varepsilon^{tt}|_i - T_\varepsilon^{nn}|_i (E_\varepsilon^{nn}|_e - E_\varepsilon^{nn}|_i) - T_\varepsilon^{tn}|_i \left(\left. \frac{\partial u_\varepsilon^t}{\partial n} \right|_e - \left. \frac{\partial u_\varepsilon^t}{\partial n} \right|_i \right) \right]. \end{aligned} \quad (32)$$

where, from a simple manipulation, we obtain

$$T_\varepsilon^{tt}|_e - T_\varepsilon^{tt}|_i = K(1 - \delta) E_\varepsilon^{tt}|_i \quad (33)$$

$$E_\varepsilon^{nn}|_e - E_\varepsilon^{nn}|_i = -(1 - \delta) (E_\varepsilon^{nn}|_i + \nu E_\varepsilon^{tt}|_i) \quad (34)$$

$$\left. \frac{\partial u_\varepsilon^t}{\partial n} \right|_e - \left. \frac{\partial u_\varepsilon^t}{\partial n} \right|_i = -2(1 - \delta) E_\varepsilon^{nt}|_i \quad (35)$$

Thus, eq. (32) becomes

$$\llbracket \Sigma_\varepsilon \mathbf{n} \rrbracket \cdot \mathbf{n} = \frac{1 - \delta}{2} \left[K (E_\varepsilon^{tt}|_i)^2 + T_\varepsilon^{nn}|_i (E_\varepsilon^{nn}|_i + \nu E_\varepsilon^{tt}|_i) + 2 T_\varepsilon^{tn}|_i E_\varepsilon^{nt}|_i \right]. \quad (36)$$

Finally, considering this last result (eq. 36) in eq. (24) and substituting it in the result of the Theorem 1 (eq. 2), the topological derivative written in terms of the stress components, becomes

$$D_T(\hat{\mathbf{x}}) = -\frac{1 - \delta}{2\delta^2 K} \lim_{\varepsilon \rightarrow 0} \frac{1}{f'(\varepsilon)} \int_{\partial B_\varepsilon} \left[\delta(1 - \nu^2) (T_\varepsilon^{nn}|_i)^2 + (T_\varepsilon^{tt}|_i - \nu T_\varepsilon^{nn}|_i)^2 + 2\delta(1 + \nu)(T_\varepsilon^{tn}|_i)^2 \right]. \quad (37)$$

Let us introduce a polar coordinate system (r, θ) centered in $\hat{\mathbf{x}} \in \Omega$, then we have the following stress distribution around a circular inclusion in a two-dimensional elastic body [28]

$$\begin{aligned}
T_\varepsilon^{nn}|_{\partial B_\varepsilon} &= \frac{\delta}{(1-\nu) + \delta(1+\nu)} (\sigma_1(\mathbf{u}) + \sigma_2(\mathbf{u})) \\
&\quad + \frac{2\delta}{(1+\nu)(1+\delta\alpha)} (\sigma_1(\mathbf{u}) - \sigma_2(\mathbf{u})) \cos 2\theta + \mathcal{O}(\varepsilon), \\
T_\varepsilon^{tt}|_{\partial B_\varepsilon} &= \frac{\delta}{(1-\nu) + \delta(1+\nu)} (\sigma_1(\mathbf{u}) + \sigma_2(\mathbf{u})) \\
&\quad - \frac{2\delta}{(1+\nu)(1+\delta\alpha)} (\sigma_1(\mathbf{u}) - \sigma_2(\mathbf{u})) \cos 2\theta + \mathcal{O}(\varepsilon), \\
T_\varepsilon^{tn}|_{\partial B_\varepsilon} &= -\frac{2\delta}{(1+\nu)(1+\delta\alpha)} (\sigma_1(\mathbf{u}) - \sigma_2(\mathbf{u})) \sin 2\theta + \mathcal{O}(\varepsilon), \quad \text{with } \alpha = \frac{3-\nu}{1+\nu}, \quad (38)
\end{aligned}$$

where $\sigma_1(\mathbf{u})$ and $\sigma_2(\mathbf{u})$ are the principal stress values of the tensor $\mathbf{T}(\mathbf{u})$, associated to the original domain without inclusion Ω ($\tau = 0$ and $\varepsilon = 0$), evaluated in the point $\hat{\mathbf{x}} \in \Omega$, that is $\mathbf{T}(\mathbf{u})|_{\hat{\mathbf{x}}}$.

Substituting the asymptotic expansion given by eq. (38) in eq. (37) we observe that function $f(\varepsilon)$ must be chosen such that

$$f'(\varepsilon) = |\partial B_\varepsilon| = 2\pi\varepsilon \quad \Rightarrow \quad f(\varepsilon) = |B_\varepsilon| = \pi\varepsilon^2 \quad (39)$$

in order to take the limit $\varepsilon \rightarrow 0$ in eq. (37), where $|B_\varepsilon|$ is used to denote the measure of B_ε .

Therefore, from this choice of function $f(\varepsilon)$ shown in eq. (39), the final expression for the topological derivative becomes a scalar function that depends on the solution \mathbf{u} associated to the original domain Ω (without inclusion), that is:

- in terms of the principal stress values $\sigma_1(\mathbf{u})$ and $\sigma_2(\mathbf{u})$ of tensor $\mathbf{T}(\mathbf{u})$

$$D_T(\hat{\mathbf{x}}) = -\frac{1-\delta}{2K} \left[\frac{1-\nu}{1-\nu + \delta(1+\nu)} (\sigma_1(\mathbf{u}) + \sigma_2(\mathbf{u}))^2 + \frac{2}{1+\delta\alpha} (\sigma_1(\mathbf{u}) - \sigma_2(\mathbf{u}))^2 \right]; \quad (40)$$

- in terms of the stress tensor $\mathbf{T}(\mathbf{u})$

$$D_T(\hat{\mathbf{x}}) = -\frac{1-\delta}{2K} \left[\frac{4(1-\nu)}{1-\nu + \delta(1+\nu)} \mathbf{T}(\mathbf{u}) \cdot \mathbf{T}(\mathbf{u}) - \frac{1}{1+\delta\alpha} (\text{tr} \mathbf{T}(\mathbf{u}))^2 \right]; \quad (41)$$

- in terms of the stress $\mathbf{T}(\mathbf{u})$ and strain $\mathbf{E}(\mathbf{u})$ tensors

$$D_T(\hat{\mathbf{x}}) = -\frac{1-\delta}{4} \frac{1+\alpha}{1+\delta\alpha} \left[2\mathbf{T}(\mathbf{u}) \cdot \mathbf{E}(\mathbf{u}) - \frac{(1-\delta)(\alpha-2)}{2\delta + \alpha - 1} \text{tr} \mathbf{T}(\mathbf{u}) \text{tr} \mathbf{E}(\mathbf{u}) \right], \quad (42)$$

which was obtained from a simple manipulation considering the constitutive relation given by eq. (8) for $\tau = 0$ and $\varepsilon = 0$. Furthermore from eq.(40) it follows that D_T is negative for soft material inclusion in a hard matrix ($\delta < 1$) and positive for hard material inclusion in a soft matrix ($\delta > 1$). This means that the cost functional decreases (increases) whenever inclusions of soft (hard) material are introduced in the configuration.

Remark 2. *It is interesting to observe that if we take $\delta = 0$ in eq. (42), the final expression for the topological derivative for inclusion in terms of $\mathbf{T}(\mathbf{u})$ and $\mathbf{E}(\mathbf{u})$ becomes*

$$\begin{aligned}
D_T(\hat{\mathbf{x}}) &= -\frac{1+\alpha}{4} \left[2\mathbf{T}(\mathbf{u}) \cdot \mathbf{E}(\mathbf{u}) - \frac{\alpha-2}{\alpha-1} \text{tr} \mathbf{T}(\mathbf{u}) \text{tr} \mathbf{E}(\mathbf{u}) \right] \\
&= -\frac{2}{1+\nu} \mathbf{T}(\mathbf{u}) \cdot \mathbf{E}(\mathbf{u}) + \frac{3\nu-1}{2(1-\nu^2)} \text{tr} \mathbf{T}(\mathbf{u}) \text{tr} \mathbf{E}(\mathbf{u}), \quad (43)
\end{aligned}$$

which is the result for circular void (see, for instance, [13, 15, 22])

4. NUMERICAL RESULTS

As already mentioned in this paper, the topological derivative allow us to quantify the sensitivity of a given cost function when the domain under consideration is perturbed by introducing an inclusion. Thus, let us write eq. (2) like a Taylor series expansion, then

$$\psi(\Omega_\varepsilon \cup B_\varepsilon) = \psi(\Omega) + f(\varepsilon) D_T(\hat{\mathbf{x}}) + \mathcal{O}(f(\varepsilon)), \quad (44)$$

where $\mathcal{O}(f(\varepsilon))$ contains all higher order terms than $f(\varepsilon)$. From analysis of eq. (44), $D_T(\hat{\mathbf{x}})$ may be seen as a first order correction¹ of $\psi(\Omega)$ to obtain $\psi(\Omega_\varepsilon \cup B_\varepsilon)$, which allow us to naturally use this derivative as a descent direction in topology design algorithm. In other words, the topological sensitivity gives the information on the opportunity to introduce a non-smooth perturbation (an inclusion in this particular case). Therefore, we may devise a topology design algorithm, based on the topological derivative given by eqs. (40, 41 or 42), which allows to simultaneously remove and insert material. Thus, let us define the parameters α , β and v_j as:

- α rate change of *hard* to *soft* material;
- β rate change of *soft* to *hard* material;
- v_j volume fraction of *hard* material at iteration j .

Let $\gamma = 1 - \alpha - \beta$, then

$$v_{j+1} = \gamma v_j + \beta \quad (45)$$

Also, we define N as the total number of iterations, thus v_N is the volume constraint of *hard* material, that is

$$v_N = |\hat{\Omega}|/|\Omega| \quad (46)$$

where $|\hat{\Omega}|$ is the required volume of hard (bulk) material. The recursive formula (eq. 45) may be written, for $0 < \gamma < 1$, as

$$\begin{aligned} v_N &= (v_0\gamma + \beta)\gamma^{N-1} + \beta \sum_{j=0}^{N-2} \gamma^j \\ &= \frac{\gamma^N [\beta + v_0(\gamma - 1)] - \beta}{\gamma - 1}. \end{aligned} \quad (47)$$

Remark 3. For the particular cases $v_0 = 0$ and $v_0 = 1$, eq. (47) becomes

$$v_N|_{v_0=1} = \frac{\alpha\gamma^N + \beta}{\alpha + \beta} \quad \text{and} \quad v_N|_{v_0=0} = \frac{(1 - \gamma^N)\beta}{\alpha + \beta}. \quad (48)$$

Remark 4. The limit $N \rightarrow \infty$, results

$$v_\infty = \frac{\beta}{1 - \gamma} = \frac{\beta}{\alpha + \beta}, \quad (49)$$

which is independent of the initial volume constraint v_0 . Therefore, if $\alpha = \beta$, $v_\infty = 1/2$.

The behavior of volume fraction v_j given by eq. (47) is shown in Fig.2.

For practical situation $N < \infty$ and $0 \leq v_0 \leq 1$. Thus, given the maximum number of iterations N , the volume constraint v_N , the rate α and the initial volume constraint v_0 , we can solve the non-linear equation given by eq. (47) for β . Let us propose a very simple fixed-point algorithm;

$$\beta_{k+1} = \frac{\gamma_k^N [\beta_k(1 - v_0) - v_0\alpha] + \alpha v_N}{1 - v_N} \quad (50)$$

with $\beta_0 = \alpha$ and $\gamma_k = 1 - \alpha - \beta_k$. This algorithm converges in a few iterations even without relaxation and it gives an estimate for β to obtain the volume constraint v_N at iteration N .

Then, with the above convergent serie (eq. 47) and the estimate for parameter β (eq. 50), the proposed algorithm may be summarized in the following steps:

¹For high order corrections see [27].

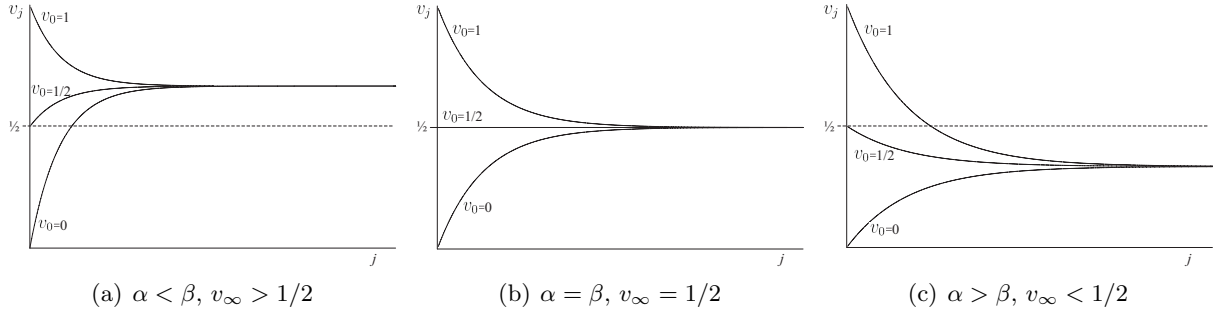


FIGURE 2. Behavior of volume fraction v_j in relation to iteration j .

- **Provide** the initial domain Ω , the required volume of hard material $|\hat{\Omega}|$, the rate change material α (hard to soft), the maximum number of iterations N and the tolerance tol .
- **Compute** the rate change material β (soft to hard).
- **While** $|\psi(\Omega^{j+1}) - \psi(\Omega^j)| > tol$ **do**:
 - : **Compute** $D_T^j(\hat{\mathbf{x}})$ in Ω
 - : **Interchange** the material property, according to $D_T^j(\hat{\mathbf{x}})$ and the parameters α and β , considering the following rule:
 - : $K \leftarrow \delta K$ in Ω^j (hard to soft)
 - : $K \leftarrow K/\delta$ in $\Omega - \Omega^j$ (soft to hard)
 - : **Set** $\Omega^{j+1} = \Omega^j$ and $j \leftarrow j + 1$.
- **Ensure** $|\Omega^j| \approx |\hat{\Omega}|$, where $|\Omega^j|$ is the volume of the hard material at iteration j .

The topological derivative depends on the solution \mathbf{u} and its gradient. In this work, the displacement field \mathbf{u} is calculated via Finite Element Method and its gradient is obtained by a post-processing technique. More specifically, the three node triangular finite element is adopted for the discretization of the variational problem. Furthermore, $D_T(\hat{\mathbf{x}})$ is evaluated at the nodal points $\hat{\mathbf{x}}_K$ of the finite elements mesh. Then the material property associated to the elements that share the node $\hat{\mathbf{x}}_K$ will be changed, as shown in Fig. 3. For more sophisticated topology algorithm based on the topological derivative see, for instance, [2, 16, 31].

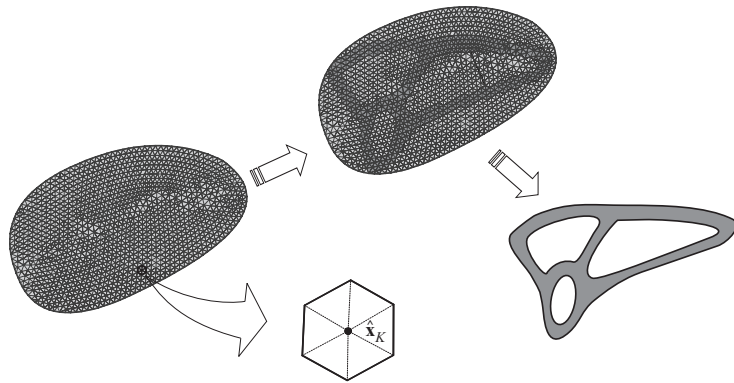


FIGURE 3. Sketching of the procedure to change the material property in a finite element mesh.

Next, we present some numerical results related to structural topology design using the above methodology. In all the examples the material properties used are given by $K = 210 \times 10^3 MPa$, $\nu = 1/3$ and $\delta = 0.01$.

4.1. **Example 1.** In this first example, the design of a bar is performed. This bar is submitted to a distributed load $\bar{q} = 250 \times 10^3 N/m$, acting in the half part of each side. In Fig. 4(a) is shown the

initial domain given by a rectangular panel with $L = 30mm$, $H = 30mm$ and $\rho = 1mm$, which is discretized taking into account the symmetry of the problem.

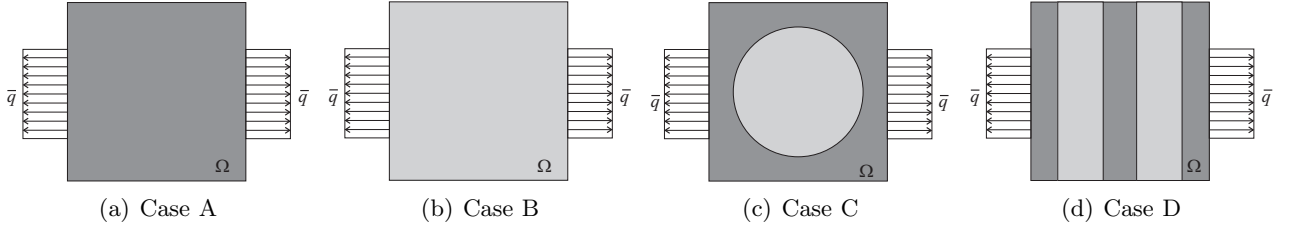


FIGURE 4. Example 1 - models and studied cases.

We consider four different initial guess. The first one (Case A) has 100% of hard material, as shown in Fig. 4(a). The second (Case B) has 100% of soft material, Fig. 4(b). The next two have 50% of hard material, where the soft part is circular for the first case (Case C) and in two equal strips for the last one (Case D), as can be seen in Figs. 4(c) and 4(d), respectively. The volume constraint used in this example are $|\hat{\Omega}| = 0.50 |\Omega|$ for Case A and B, and $|\hat{\Omega}| = |\Omega|$ for the last two cases (C and D). Then, at the end of the iterative process, all cases have 50% of hard material. Finally, the rate of material to be changed at each iteration is given for $\alpha = 0.01 |\Omega^j|$.

In the next sequence of figures (Fig. 5 to Fig. 8) four steps are shown, for each studied case, of the iterative process described by the topology algorithm introduced at the beginning of this section. The mentioned steps correspond to iterations $j \in \{40, 80, 120, 160\}$.

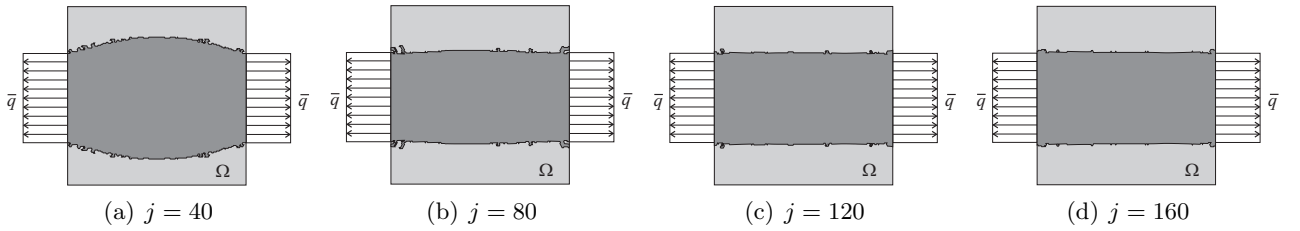


FIGURE 5. Example 1 - iterative process for case A.

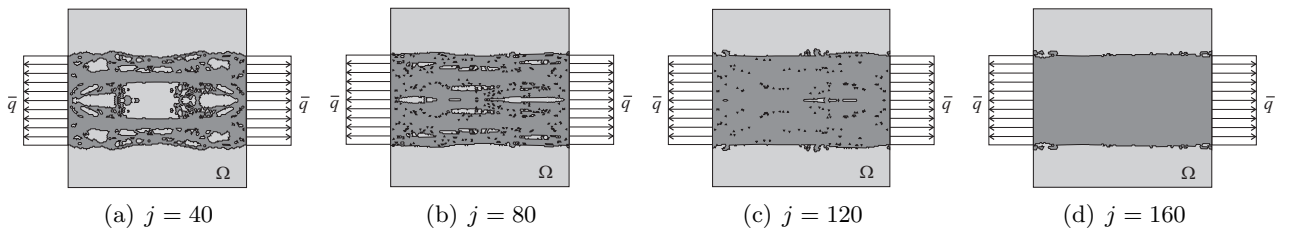


FIGURE 6. Example 1 - iterative process for case B.

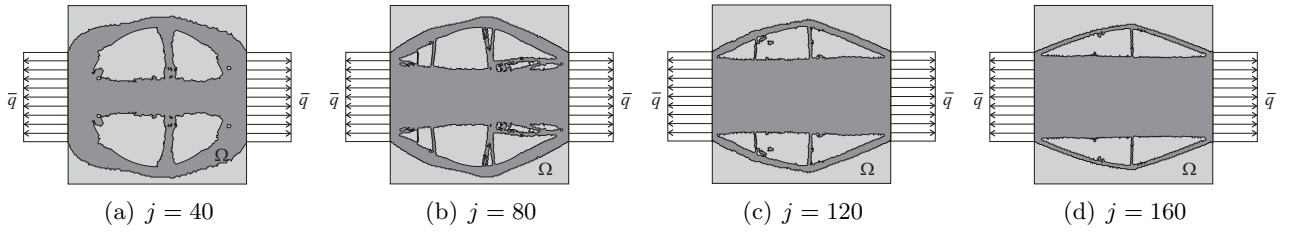


FIGURE 7. Example 1 - iterative process for case C.

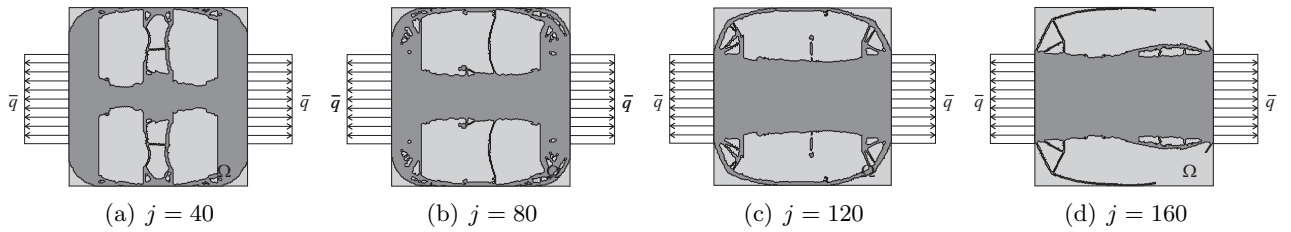
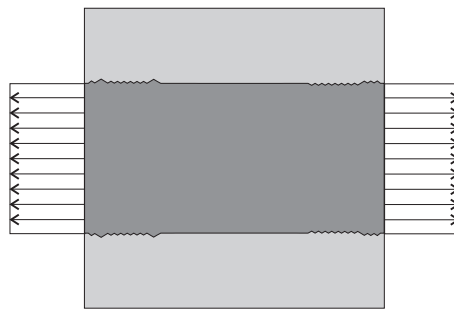


FIGURE 8. Example 1 - iterative process for case D.

The final topology shown in Fig. 9, obtained at iteration $j = 200$, is the same for all cases. Therefore, the proposed algorithm is able to find global minimum independent of the initial guess, at least for this simple example.

FIGURE 9. Example 1 - obtained topology at $j = 200$.

The cost function $\psi(\Omega^j)$ and the volume of the hard material $|\Omega^j|$ throughout the iterative process are respectively shown in Figs. 10(a) and 10(b), where $\psi(\Omega^*)$ is the cost function associated to the optimal domain Ω^* .

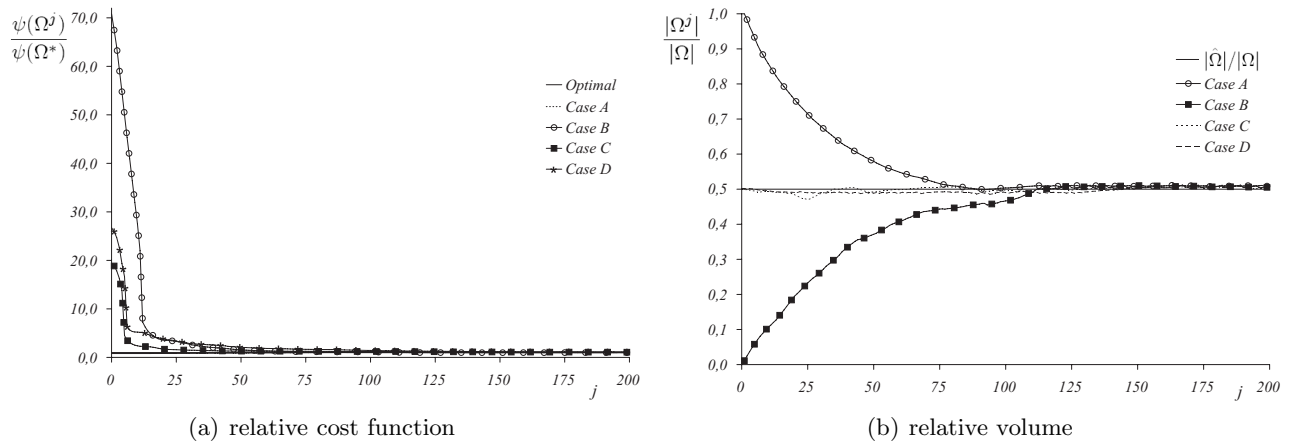


FIGURE 10. Example 1 - obtained results.

4.2. Example 2. The design of a Mitchell structure is performed. In Fig. 11(a) is shown the initial domain given by a simply supported rectangular panel with $L = 100mm$, $H = 50mm$ and $\rho = 5mm$, submitted to a concentrated load $\bar{Q} = 5000N$ on the bottom. Due to the symmetry of the problem, only half of the panel is discretized.

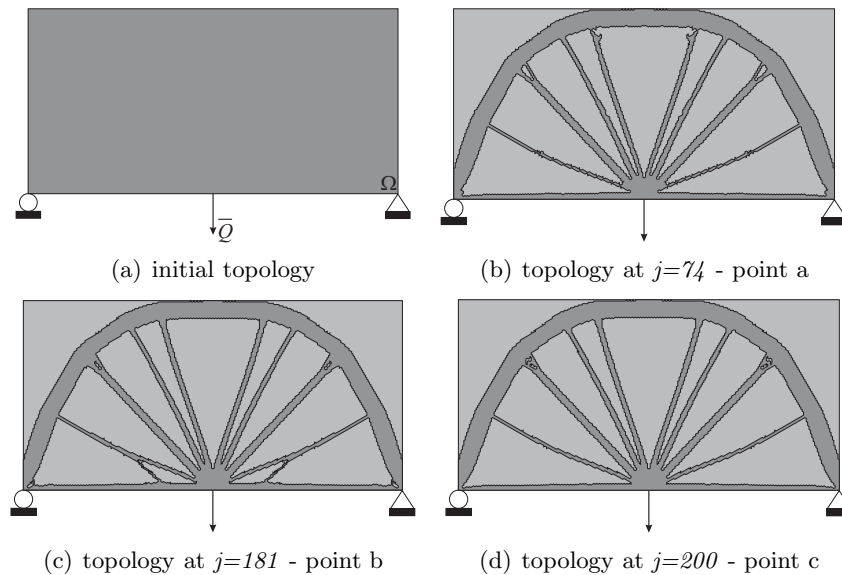


FIGURE 11. Example 2 - model and obtained topologies.

Taking $|\hat{\Omega}| = 0.25 |\Omega|$ and $\alpha = 0.01 |\Omega^j|$, we have $|\Omega^j| \approx |\hat{\Omega}|$ for $j = 74$, whose topology is shown in Fig. 11(b). Once the volume constraint is reached, we consider $\alpha = 0.0025 |\hat{\Omega}|$. The results obtained at $j = 181$ and $j = 200$ are respectively shown in Figs. 11(c) and 11(d). The cost function $\psi(\Omega^j)$ and the volume of the hard material $|\Omega^j|$ are presented in Figs. 12(a) and 12(b), respectively.

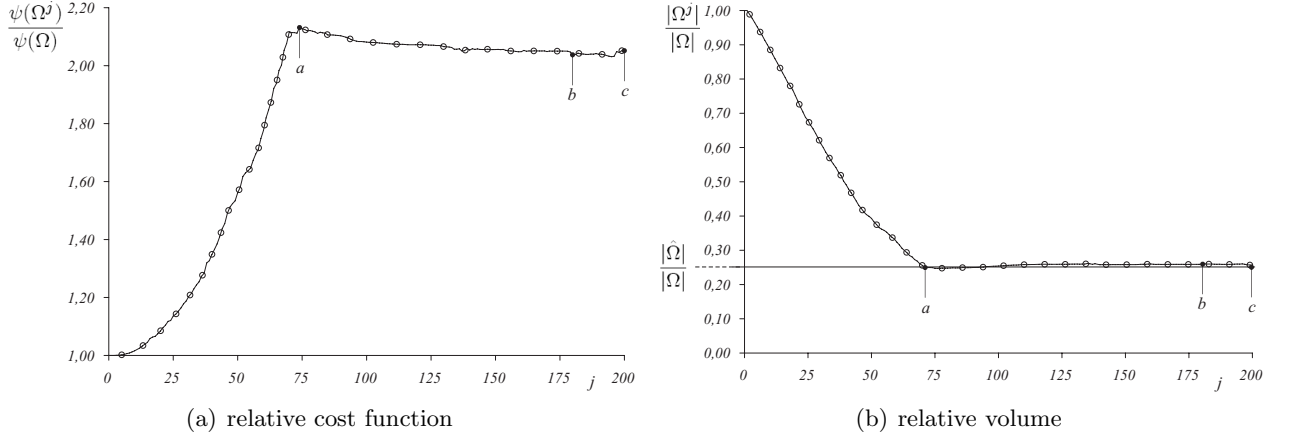


FIGURE 12. Example 2 - obtained results.

4.3. Example 3. Now, in this third example, we consider the design of two bridges. In both cases the initial domain is represented by a rectangular panel with $L = 180m$, $H = 60m$ and $\rho = 0.3m$, submitted to a uniformly distributed traffic loading $\bar{q} = 250 \times 10^3 N/m^2$. This load is applied on the black strip of height $b = 3m$, which is positioned at distance c from the top of the design domain. Taking into account the symmetry of both problems, only half part of the domain will be discretized. **Case A:** the initial domain is clamped on the region $a = 9m$ and the strip is positioned at $c = 30m$, as can be seen in Fig. 13(a). Taking $|\hat{\Omega}| = 0.25 |\Omega|$ and $\alpha = 0.01 |\Omega^j|$, the topology obtained at iteration $j = 94$ is shown in Fig. 13(b), where $|\Omega^j| \approx |\hat{\Omega}|$. Next, we consider $\alpha = 0.0025 |\hat{\Omega}|$ and the obtained results are presented in Fig. 13(c) ($j = 350$).

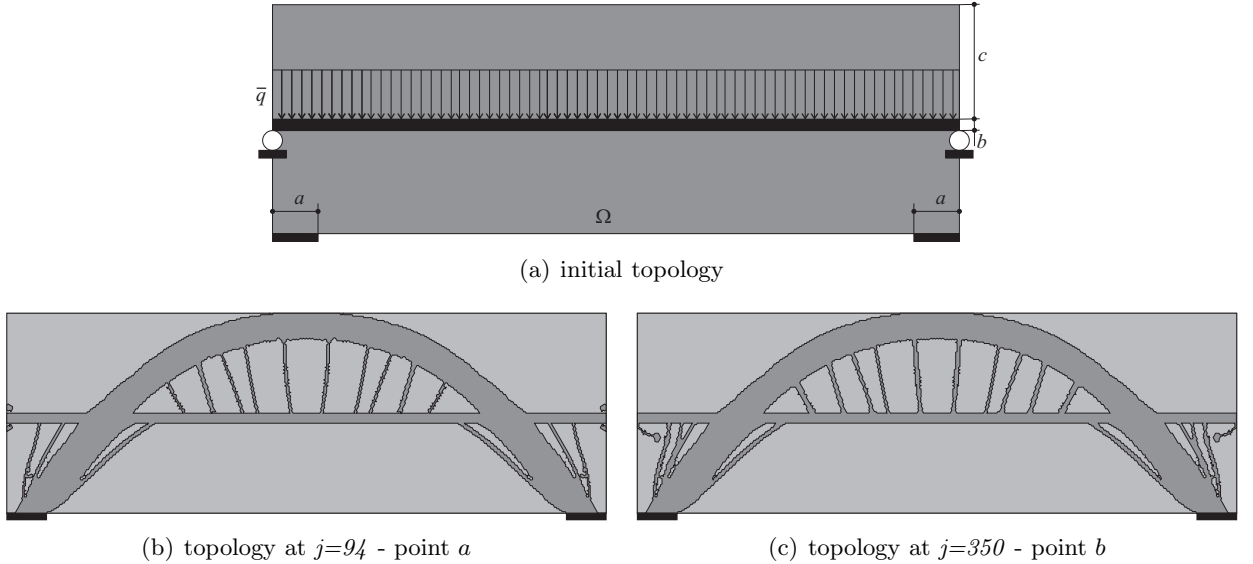


FIGURE 13. Example 3 (Case A) - model and obtained topologies.

Case B: the initial guess is simply supported on the region $a = 9m$ and the parameter c is given by $c = 57m$, as shown in Fig.14(a). Considering again $|\hat{\Omega}| = 0.25 |\Omega|$ and $\alpha = 0.01 |\Omega^j|$, the topology obtained at iteration $j = 83$, where $|\Omega^j| \approx |\hat{\Omega}|$, is presented in Fig. 14(b). Now, we take $\alpha = 0.0025 |\hat{\Omega}|$ and the result reached at iteration $j = 350$ is shown in Fig. 14(c).

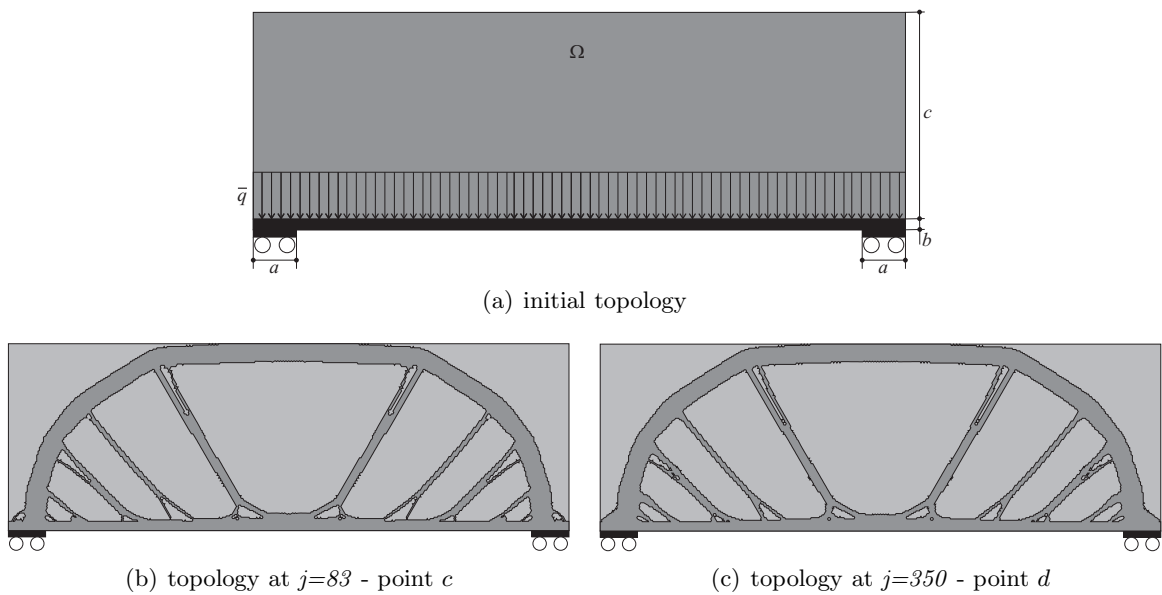


FIGURE 14. Example 3 (Case B) - model and obtained topologies.

In the last figure of this work, Fig. 15, we present a comparison between the cost function $\psi(\Omega^j)$ for both cases obtained throughout the iterative process.

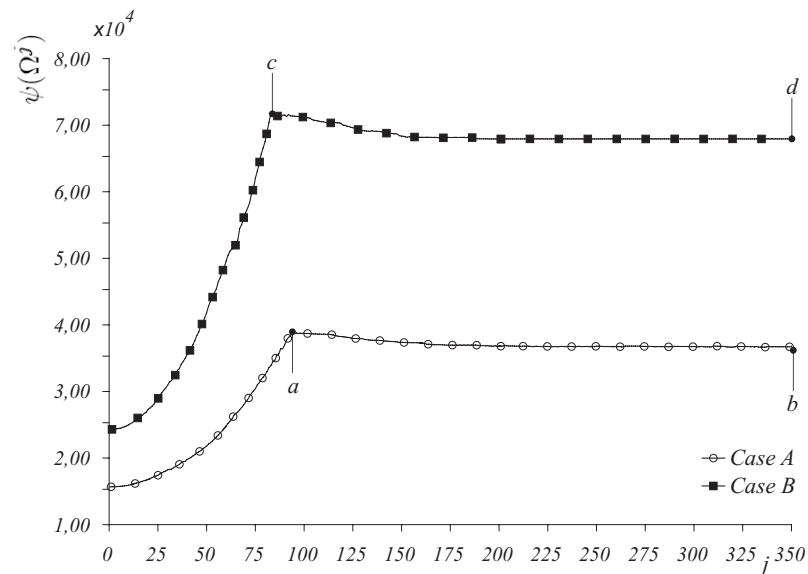


FIGURE 15. Example 3 - cost function.

Finally, it is important to note that the final topologies obtained, in both cases, coincide with the classical result of a tied arch bridge structure, as it was expected (see Figs. 13(c) and 14(c)).

5. CONCLUSIONS

In this work, we have applied the Topological-Shape Sensitivity Method to calculate the topological derivative for inclusion in two-dimensional linear elasticity problem taking the total potential energy as the cost function and the state equation in its weak form as the constraint. The explicit formula for the topological derivative, given by eqs. (40,41,42), was obtained using classical asymptotic analysis around circular inclusions. The obtained result was used to devise a topology design algorithm which

allows to simultaneously remove and insert material. This feature is very important to find global or, at least more than one local minimum. In fact, we have shown through the numerical experiments that the proposed algorithm is able to find global minimum independent of the initial guess (example 1) and also several local minima (examples 2 and 3).

ACKNOWLEDGMENTS

We would like to thank Professors Raúl Feijóo and Edgardo Taroco for many helpful and stimulating discussions and for their careful review of this manuscript. This research was partly supported by the Brazilian agencies CNPq/FAPERJ-PRONEX (E-26/171.199/2003) and by CONICET (Argentina). Sebastián Miguel Giusti was partially supported by Brazilian government fellowship from CAPES. The support from these agencies is greatly appreciated.

REFERENCES

- [1] S. Amstutz. *Aspects théoriques et numériques en optimisation de forme topologique*. Ph. D. Thesis, Institut National des Sciences Appliquées de Toulouse, France, 2003.
- [2] S. Amstutz & H. Andrä. A new algorithm for topology optimization using a level-set method. *Research Report*, Université Paul Sabatier, Toulouse Cedex 4, France, 2005.
- [3] S. Amstutz, I. Horchani & M. Masmoudi. Crack detection by the topological gradient method. *Control and Cybernetics*, **34(1)**:119-138, 2005.
- [4] D. Auroux, M. Masmoudi & L. Belaid. Image restoration and classification by topological asymptotic expansion. *Variational Formulations in Mechanics: Theory and Applications* - CIMNE, Barcelona, Spain, 2006.
- [5] L.J. Belaid, M. Jaoua, M. Masmoudi & L. Siala. Application of the topological gradient to image restoration and edge detection. To appear on *Engineering Analysis with Boundary Element*, 2007.
- [6] M. Bonnet. Topological sensitivity for 3D elastodynamic and acoustic inverse scattering in the time domain. *Computer Methods in Applied Mechanics and Engineering*, **195(37-40)**:5239-5254, 2006.
- [7] M. Bonnet, A. Constantinescu. Inverse problems in elasticity. *Inverse Problems*, **21(2)**:R1-R50, 2005.
- [8] J. Céa, S. Garreau, Ph. Guillaume & M. Masmoudi. The Shape and Topological Optimizations Connection. *Computer Methods in Applied Mechanics and Engineering*, **188**:713-726, 2000.
- [9] H.A. Eschenauer, V.V. Kobelev & A. Schumacher. Bubble Method for Topology and Shape Optimization of Structures. *Structural Optimization*, **8**:42-51, 1994.
- [10] H.A. Eschenauer & N. Olhoff. Topology Optimization of Continuum Structures: A Review. *Applied Mechanics Review*, **54**:331-390, 2001.
- [11] J.D. Eshelby. The Elastic Energy-Momentum Tensor. *Journal of Elasticity*, **5**:321-335, 1975.
- [12] R.A. Feijóo, A.A. Novotny, E.A. Taroco & C. Padra. The Topological Derivative for the Poisson's Problem. *Mathematical Models and Methods in Applied Sciences*, **13-12**:1-20, 2003.
- [13] R.A. Feijóo, A.A. Novotny, C. Padra & E.A. Taroco. The Topological-Shape Sensitivity Method and its Application in 2D Elasticity. To appear on *Journal of Computational Methods in Sciences and Engineering*, 2007.
- [14] G.R. Feijóo. A new method in inverse scattering based on the topological derivative. *Inverse Problems* **20(6)**:1819-1840, 2004.
- [15] S. Garreau, Ph. Guillaume & M. Masmoudi. The Topological Asymptotic for PDE Systems: The Elasticity Case. *SIAM Journal on Control and Optimization*, **39**:1756-1778, 2001.
- [16] X. Guo, K. Zhao & M.Y. Wang. A New Approach for Simultaneous Shape and Topology Optimization Based on Dynamic Implicit Surface Function. *Control and Cybernetics*, **34(1)**:255-282, 2005.
- [17] M.E. Gurtin. *An Introduction to Continuum Mechanics*. Mathematics in Science and Engineering vol. 158. Academic Press, 1981.
- [18] M.E. Gurtin. *Configurational Forces as Basic Concept of Continuum Physics*. Applied Mathematical Sciences vol. 137. Springer-Verlag, 2000.
- [19] B.B. Guzina & M. Bonnet. Small-inclusion asymptotic of misfit functionals for inverse problems in acoustics. *Inverse Problems* **22(5)**:1761-1785, 2006.
- [20] I. Larrabide, R.A. Feijóo, A.A. Novotny & E.A. Taroco. Topological Derivative: A Tool for Image Processing. To appear on *Computers & Structures*, 2007.
- [21] I. Larrabide. *Processamento de Imagens via Derivada Topológica e suas Aplicações na Modelagem e Simulação Computacional do Sistema Cardiovascular Humano*. Ph. D. Thesis, LNCC/MCT, Petrópolis - RJ, Brazil, 2007.
- [22] T. Lewiński & J. Sokolowski. Energy change due to the appearance of cavities in elastic solids. *International Journal of Solids and Structures*, **40**:1765-1803, 2003.
- [23] M. Masmoudi, J. Pommier & B. Samet. The topological asymptotic expansion for the maxwell equations and some applications. *Inverse Problems*, **21**:547-564, 2005.
- [24] F. Murat & J. Simon. *Sur le Contrôle par un Domaine Géométrique*. Thesis, Université Pierre et Marie Curie, Paris VI, France, 1976.

- [25] A.A. Novotny. *Análise de Sensibilidade Topológica*. Ph. D. Thesis, LNCC/MCT, Petrópolis - RJ, Brazil, 2003.
- [26] A.A. Novotny, R.A. Feijóo, C. Padra & E.A. Taroco. Topological Sensitivity Analysis. *Computer Methods in Applied Mechanics and Engineering*, **192**:803-829, 2003.
- [27] J. Rocha de Faria, A.A. Novotny, R.A. Feijóo, E.A. Taroco & C. Padra. Second Order Topological Sensitivity Analysis. *International Journal of Solids and Structures*, **44**(14-15):4958-4977, 2007.
- [28] M.A. Sadowsky & E. Sternberg. Stress Concentration Around a Triaxial Ellipsoidal Cavity. *Journal of Applied Mechanics*, 149-157, 1949.
- [29] J. Sokolowski & A. Żochowski. On the Topological Derivative in Shape Optimization. *SIAM Journal on Control and Optimization*, **37**:1251-1272, 1999.
- [30] E.A. Taroco, G.C. Buscaglia & R.A. Feijóo. Second-Order Shape Sensitivity Analysis for Nonlinear Problems. *Structural Optimization*, **15**:101-113, 1998.
- [31] M. Yulin & W. Xiaoming. A level set method for structural topology optimization and its applications, *Advances in Engineering Software*, **35**:415-441, 2004.

(S.M. Giusti) LABORATÓRIO NACIONAL DE COMPUTAÇÃO CIENTÍFICA LNCC/MCT, AV. GETÚLIO VARGAS 333, 25651-075 PETRÓPOLIS - RJ, BRASIL

(A.A. Novotny) LABORATÓRIO NACIONAL DE COMPUTAÇÃO CIENTÍFICA LNCC/MCT, AV. GETÚLIO VARGAS 333, 25651-075 PETRÓPOLIS - RJ, BRASIL

E-mail address: novotny@lncc.br

(C. Padra) CENTRO ATÓMICO BARILOCHE, 8400 BARILOCHE, ARGENTINA